

Battery State of Charge Monitor for Internet of Things Devices

Pedro Miguel Mateus Coutinho
Instituto Superior Técnico
Lisboa, Portugal
pedro.coutinho.87733@tecnico.ulisboa.pt

Abstract— This paper describes a state of charge measurement system designed for batteries of Internet of Things devices. This new circuit has an integrator and a transistor that replace an ADC from the conventional Coulomb counting method. The main objective of this component replacement is to study another way of measuring current without compromising the measurement's accuracy, energy consumption and production cost of the circuit of the Coulomb counting method.

The measurement of the current discharged from the battery is then used to calculate its remaining percentual charge, the state of charge. To achieve this, the voltage of the sense resistor is amplified and integrated originating a pulse signal that is digitally processed inside the microcontroller. Simultaneously, this device counts the pulses, relates them to the discharge current and instantaneously sends the state of charge value to the user interface.

Keywords— Batter; Internet of Things; State of Charge; Coulomb Counting.

I. INTRODUCTION

Between several state of charge (SOC) methods, the Coulomb counting technique is one of the most accurate techniques, designed for all types of batteries, convenient since they don't need to be intervened and may be used simultaneously while measuring the discharged current.

Batteries are responsible for converting efficiently and safely electrical to chemical energy, and vice-versa, to power wireless Internet of Things devices. These charge storage devices depend heavily on certain factors such as: operational temperature; discharging current; safety precautions; and ease of access. Primary batteries are non-rechargeable power sources with prominence on the alkaline and lithium-iron disulfide types since these are two equally-shaped batteries.

The Internet of Things (IoT) is a set of programmed devices that interact with each other and can be accessed in real time from a remote location depending on the type of network used.

The state of charge (SOC) is a key indicator responsible for stating a percentual remaining charge capacity of a battery. There are several SOC estimation methods that measure this indicator in different ways such as: chemically; using pressure; measuring the open circuit voltage (OCV); measuring the discharged current.

To have the maximum benefit from the new measurement concept, the modified Coulomb counter was developed. Compared with the general circuit of the Coulomb counting method, this new circuit has the same two components: a sense resistor; and an operational amplifier. Between these two electronic circuits, the new method has three other components responsible for the

current integration that replace the analog-to-digital converter (ADC) of the general circuit: the resistor and capacitor responsible for the current integration; and the transistor responsible for charging and discharging the capacitor. Together, maximum error of the SOC estimation is below 3% within the current range from 1 mA up to 110 mA at 20-22°C with a production cost of 10€.

II. BATTERY CHEMISTRY

A cell is an electrochemical component that contains the electrodes, a separator, and an electrolyte while a battery is a group of cells with housing, electrical connections, and, in some cases, a protective electronic circuit [1].

The electrodes correspond to the conductive part in contact with a material of less conductivity responsible for exchanging positive or negative charge carriers. Demonstrated in Fig. 1, the electrons are the negative charge that flow from the negative to the positive electrodes, anode, and cathode, respectively. On the other hand, the electrolyte is a substance that enables the flow of these electrons, responsible for separating the anode from the cathode preventing the electrodes from being in contact with each other.

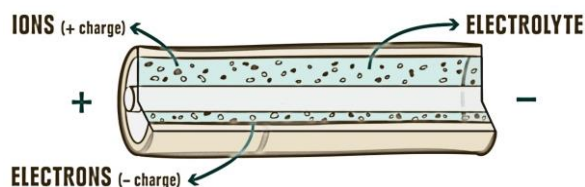


Fig. 1. Inside a common battery [5].

Batteries work in two different mechanisms, the charge and discharge mechanism. In the first, the battery receives electrical energy and converts that energy chemically to move electrons from the cathode to the anode. The second mechanism consists of an operation in which the battery supplies electrical energy by electrons from the anode to the cathode.

There are two types of voltaic batteries: primary and secondary. The primary ones are all types of non-rechargeable batteries, while the secondary ones are the batteries designed to be rechargeable. A primary battery is a galvanic battery intended for one time usage due to its non-reversible electrochemical reaction inside the battery. Several characteristics should be considered when choosing a battery such as: the initial and life-cycle costs; rechargeable or non-rechargeable; operating temperature; operating voltage; size, design, and weight.

The Fig. 2 illustrates five common battery designs and sizes used in most IoT and non-IoT devices. These letters are indicators of size and voltage output. The further moving

along the alphabet letters, the larger are these two variables and if a letter is used more than once, than the smaller it size.



Fig. 2. Illustration of the five most common batteries [6].

For example, PP3 has more voltage output than D and AAA is smaller than AA. In these five energy storage devices, only the AAA, AA and PP3 (9-Volt) batteries are specifically characterized and studied for alkaline batteries however only AA and AAA for lithium-iron due to not existing the typical 9 V lithium-iron batteries.

Devices will only function normally in a certain voltage range that they were intended to work on, so after some usage, a battery will not be able to power it normally. Certain factors can make a battery less efficient as well as affecting its lifetime: low temperatures inhibit the ions' movement and, consequently, lowers the battery's efficiency; high current drainage reduces the battery capacity because with higher current, the less time there is for the chemical reactions to occur and consequently less energy may be discharged from the battery.

A. Alkaline Batteries

An alkaline battery is composed by an alkaline potassium hydroxide (KOH) electrolyte and can be rechargeable or non-rechargeable. The cathode is a compound of magnesium dioxide (MnO_2) while the anode is zinc (Zn). Alkaline batteries are susceptible to leaking their electrolyte due to attempts on recharging, combining different battery chemistries to power the same circuit or storing batteries in humid places with peak temperatures.

Although high discharge currents have a severe impact on alkaline batteries, these devices are typically used for devices that generally have low supply current and where certain factors such as weight, size and energy density are not deal breakers.

B. Lithium Iron Disulfide Batteries

In this project, lithium iron disulfide ($LiFeS_2$) batteries are studied for being very similar to alkaline cells since they are disposable and share the same shapes and sizes. Lithium is the lightest and most active metal and, when in contact with iron disulfide, it can supply the energy needed for most electronic devices with a nominal voltage of 1.5 V for AA and AAA batteries.

The non-aqueous electrolyte of these batteries is designed to work with wide temperature ranges from $-40^\circ C$ to $60^\circ C$ [2]. Like the alkaline batteries, the voltage of the lithium metal ones also gradually reduces over time once the resources responsible for the chemical reaction are depleted.

Lithium iron disulfide batteries are less sensitive to temperature than alkaline though the service life is still affected if the temperature is lowered below room temperature ($20^\circ C$) [2].

TABLE I. BATTERIES' COMPARISON [2].

Characteristics	Battery Type	
	Lithium-iron	Alkaline
Cold Temperature Performance	Superior	Good
Weight	33% < Alkaline	33% > Lithium
Shelf Life	20+ Years	5 to 10 Years
Leakage	Superior	Good
Discharge Curve	Flat	Sloping
High Rate Capability	Superior	Good
Safety	Concerning	Safe
Price	High	Low

III. STATE OF CHARGE

The state of charge (SOC) is the level of charge remaining in a battery and it is the quotient between the amount of payload and the total capacity of the battery. The payload, $Q(t)$, is the total amount of charge remaining in a battery and, Q_n , is a pre-determined value considered as the minimum usable [3]. The SOC is expressed as a percentage,

$$SOC(t) = \frac{Q(t)}{Q_n} \times 100 [\%]. \quad (1)$$

Generally, there are four common SOC estimation techniques that may be used depending on the types of applications required: Chemical; Voltage; Pressure; Coulomb counter.

A. Coulomb Counting Method

The Coulomb counting is the approach that is the most used and the one chosen for this project as it is easily implemented and directly applied method for measuring and integrating the battery's discharging current over time given by,

$$SOC(t) = SOC(t-1) + \frac{I(t)}{Q_n} \Delta t \quad (2)$$

Where $SOC(t-1)$ represents the previous estimated value of SOC, Q_n is the totally charged capacity and $I(t)$ is the discharging current. The Coulomb counting procedure calculates the SOC by accumulating the value of the sourced charge and its accuracy depends mostly on the sampling accuracy and the current sensor's frequency. The SOC is estimated by integrating the charging and discharging currents, initially knowing, or estimating its' value. There are always losses and inaccuracies during charge and discharge processes as the output charge is always less than the stored charge. There are some factors that influence the inaccuracy of the Coulomb counting approach including the battery's temperature, history, discharge current, and life-cycle [4].

The conventional Coulomb charging method measures the SOC by measuring the current flowing in the Rsense resistor with the analog to digital converter (ADC) and storing it with the accumulator and real-time clock (RTC). Comparing this value with the knowing starting point, the SOC can be estimated.

B. Coulomb Integrator Approach

An improved technique of the conventional method is proposed with the following circuit represented in Fig. 3. This new approach, Coulomb Integrator, is composed by a NMOS Field Effect Transistor (FET) M1, a capacitor C1, a resistor R1 an operational amplifier (Op-amp) and a Microcontroller MSP430FR2311. In this approach, the SOC is estimated by measuring the current flowing in the Rsense, amplifying the signal with Op-amp, integrating it using a low-pass filter, and comparing the signal with a predefined.

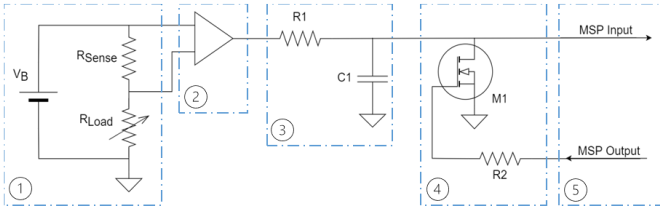


Fig. 3. Proposed Coulomb counting method.

The first block of this circuit exemplifies a device powered by the battery connected to a sense resistor, Rsense, that must have a significantly lower value compared to the load's impedance because the higher the Rsense impedance, the lower the voltage on the load.

Represented in the second block, the Operational Amplifier (Op-Amp) to prevent any influence on the sense and load circuits from the following stages of the architecture, but also for amplifying the Rsense voltage signal that is directly proportional to the desired current value.

For example, when the load is being sourced with two 1.5 V battery's discharging 100 mA, on the first block, the voltage of the Rsense, Vs, is approximately equal to 27 mV and the load's voltage is the subtraction between these two: 2.973 V. Then, in the second block, the Op-Amp has one of the reference voltages connected to ground and the other Vref connected to the microcontroller's 3.3 V. Thus, the output of the Op-Amp is equal to 1.65 V for a 0 V input, half the microcontroller's voltage supply, and 3.3 V for a maximum of 82.5 mV input.

The third block are the components accountable for integrating the voltage originating a sawtooth waveform output. The transistor M1 from the fourth block is used for discharging the integrator. Demonstrated in Fig. 4, when the Microcontroller's output is LOW, the capacitor charges and, while it charges, the value of the capacitor's voltage is compared with 1 V inside the Microcontroller. When this input value reaches the compared voltage value, the MSP's output is HIGH, and the transistor discharges the capacitor.

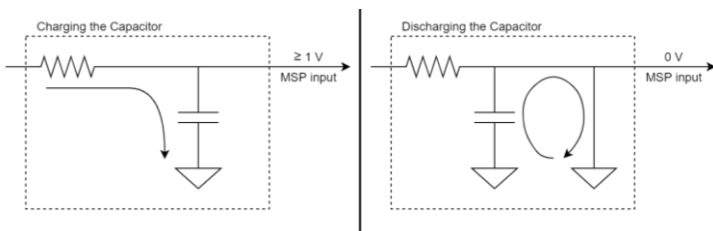


Fig. 4. Transistor charging and discharging the capacitor illustration.

For example, if the discharge current is 110 mA, the voltage at the sense resistor is around 30 mV. After amplifying the signal, the Op-Amp's output voltage, Vop is equal to,

$$V_{op} = 1.65 + 20 \times V_s = 2.25 \text{ V} \quad (3)$$

In Fig. 5, the values of the voltage of the resistor and capacitor are illustrated in yellow and blue, respectively, which characterize the voltage of the components of the integrator from the third block while charging the capacitor.

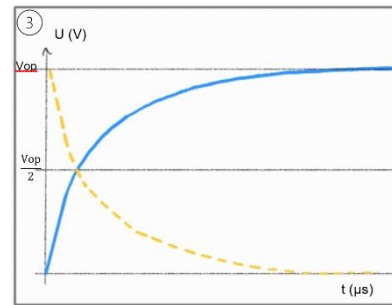


Fig. 5. Voltage output signal representation of block 3 with 100 mA.

Then, the Fig. 6 is an illustration of the influence of the fourth block since the microcontroller compares the capacitor's voltage in yellow with 1 V, the transistor discharges it every time it reaches this compared V1 value and consequently outputting the sawtooth signal represented in blue.

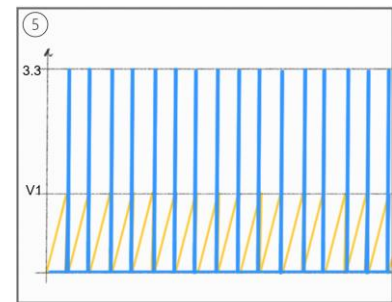


Fig. 6. Voltage output signal representation of block 4 with 100 mA.

After the fourth block, illustrated in Fig. 7, the fifth block represents the MSP I/O ports that are connected to the circuit. The yellow line is the input signal of the MSP, and it is connected to one of the comparator's inputs. This internal enhanced comparator (eCOMP) outputs a HIGH voltage, 3.3 V, whenever the input is higher than the comparing value of 1 V, V1, and outputs a LOW voltage, 0 V, whenever it is lower, generating an equivalent pulsed signal represented in blue.

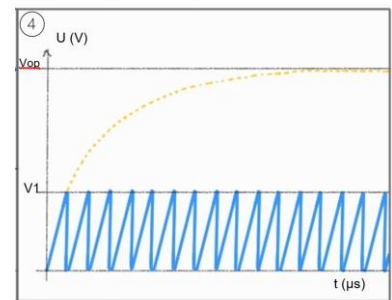


Fig. 7. Voltage output signal representation of block 5 with 100 mA.

However, if the discharge current is 1 mA, the voltage at the sense resistor is equal to $270 \mu\text{V}$. After amplifying the signal, the Op-Amp's output voltage, V_{op}' is equal to,

$$V_{op}' = 1.65 + 20 \times V_s = 1.66 \text{ V} \quad (4)$$

Therefore, as show in Fig. 8 of the 1 mA discharge example, in block 4 the yellow line shows the capacitor taking more time to charge completely and, consequently, in blue, the charge until reaching 1 V takes longer than when the battery was discharging at 100 mA.

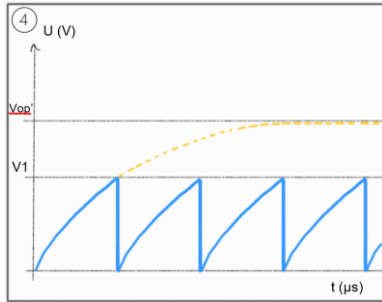


Fig. 8. Voltage output signal representation of block 4 with 1 mA.

Accordingly, as for block 5, illustrated in Fig. 9 the microcontroller's output pulses are more spaced out between each HIGH output meaning that the counter will count less pulses in the same period compared to the 100 mA discharge.

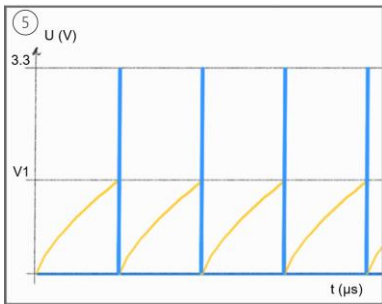


Fig. 9. Voltage output signal representation of block 5 with 1 mA.

Comparing the fifth blocks of the Fig. 7 and Fig. 9, it can be assumed that the higher the value of the discharge current, the higher the number of pulses and the lower the duration between pulses for the same period. The goal of the project's implemented approach is to exhibit the correct functioning of this architecture since the integrator outcome resembles an analog-to-digital converter (ADC).

IV. COULOMB INTEGRATOR

This project is designed to work for current measures between 1 mA and 110 mA for better precise and accurate measurements. The implemented Coulomb Integrator integrates the amplified signal by comparing it with a reference voltage and discharging the capacitor whenever this voltage is reached originating a pulsed signal. The greater the Op-Amps output voltage, the greater the current that passes through the capacitor and, consequently, the faster it charges. Because the Op-Amp's output is between the range of 1.65 and 3.3 Volts and the comparator's reference voltage is 1 V, the signal is continuously being integrated and, consequently, there is always a minimum and maximum range of pulses per second. The Table II shows the range of the oscillating frequency (number of

pulses per second), duration between pulses, and the corresponding Op-Amp's output voltages. The shorter the duration between these pulses, the higher the current and vice-versa.

TABLE II. VARIABLES BETWEEN DIFFERENT CURRENTS.

Discharged Current (mA)	Op-Amp Output Voltage (V)	Oscillating Frequency (Hz)	Duration Between Pulses (ms)
306	3.3	87	11.5
110	2.25	54	18.5
1	1.66	34	29.4

Then, having acquired the time between pulses, this time was directly related to the current using a look-up table with 128 steps of current accuracy between 1 and 110 mA of current range.

A. Circuit's Assembly and Configuration

The comparator is one of the most important components of the circuit being one of the key reasons why the MSP430FR2311 was chosen since not all microcontrollers have this internal comparator. Firstly, the comparator's input pin is connected to the resistor that connects the amplifier's output to the capacitor's anode and the transistor's collector pins, illustrated in Fig. 10.

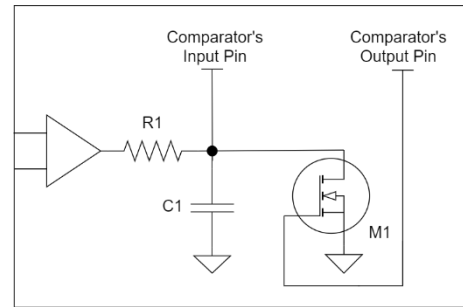


Fig. 10. Comparator's input and output pins.

Then, in the code, it is used a DAC buffer that states the voltage comparison value on the other comparator's input pin. The comparator's reference voltage and the integrator's impedance and capacity's values were chosen in way that the relationship between the oscillating frequency and the current was as linear as possible and where the current values were more easily distinguished. For this matter, it was chosen a 1 V as the comparator's DAC reference, a 100 kΩ impedance and 330 nF capacitance.

If the capacitor voltage is lower than this value, the comparator output is LOW causing the transistor not to discharge the capacitor and the interruption stays disengaged. On the other hand, if the values are higher than the comparison voltage, as soon as it activates the port, the transistor starts to conduct, the integrator discharges and the comparator's output goes back to zero.

An interruption is needed so that the value of the timer's variable can be retained and reset for calculating the duration between the impulses. Since the MSP430FR2311 microcontroller does not have the printf function, UART communication must be used to perform character by character communication.

B. SOC Estimation

For comparison and validation, two methods were made to verify the SOC measured by the circuit: voltage and capacity discharge comparisons.

The first method, SOC_1 , was to compare the voltage acquired by the DAQ, V_{DAQ} , with the range of the battery's nominal voltage, V_n , and discharged voltage, V_d . The voltage of a battery decreases with use, and it won't work properly below the discharged voltage stated in the manufacturer's datasheet. Therefore, the nominal voltage is set as the 100% battery's SOC reference and the discharged voltage as the 0% empty charge,

$$SOC_1 (\%) = \frac{(V_{DAQ} - V_d) (V)}{(V_n - V_d) (V)} \quad (5)$$

The main drawback of this method is for not being precise since the battery's voltage decreases more when reaching the discharged voltage value than between these two references. In that matter, the second method, SOC_2 , takes place by calculating the ratio of the discharged capacity from the battery, C_d , and the nominal capacity, C_n , stated by its manufacturer,

$$SOC_2 (\%) = \frac{C_d (\text{mAh})}{C_n (\text{mAh})} \quad (6)$$

Although being precise, this method won't work if the discharged current is unknown, or it wasn't constant in all the acquisition time since the discharged capacity can only be calculated knowing the discharged current, I_d , and the acquisition time, t_a ,

$$C_d (\text{mAh}) = I_d (\text{mA}) \times t_a (\text{h}) \quad (7)$$

During acquisitions, the current requested from the battery varied as the voltage of the battery varies with use. However, as the initial and final current values can be known by calculating the ratio of the battery's voltage with the known constant impedance, the current used can be estimated and, consequently, the capacity that has been removed from the battery is determined,

$$I_d (\text{mA}) = \frac{(V_n + V_{DAQ}) (\text{mV})}{2 \times R (\Omega)} \quad (8)$$

V. VALIDATION RESULTS

The data acquired from the microcontroller and the DAQ device were gathered and graphically displayed for validation of the project's measurements. The goal is to compare alkaline and lithium iron disulfide batteries' behaviors exposed to different operational temperatures or to high discharging currents. To validate these results, the graphs were compared to the datasheet of the batteries' manufacturer and to the voltage measurement acquired with the DAQ device.

Although AAA, AA and 9 V alkaline batteries have an approximate capacity of 1200 mAh, 2900 mAh and 650 mAh, respectively, the nominal capacity of these batteries varies significantly depending on the discharge current. Comparing these alkaline batteries, AA batteries are more dependent on the discharge current than AAA and the 9 V

batteries are less dependent on the required current than AAA. This means, for example, with a 110 mA current discharge, an alkaline AAA battery of 1200 mAh nominal capacity has a real capacity of approximately 926 mAh. Based on the datasheet provided by the manufacturer of these three types of batteries, functions were made to adjust the values of their nominal capacities according to the discharged current and the SOC graphs were accurately obtain as illustrated in Fig. 11.

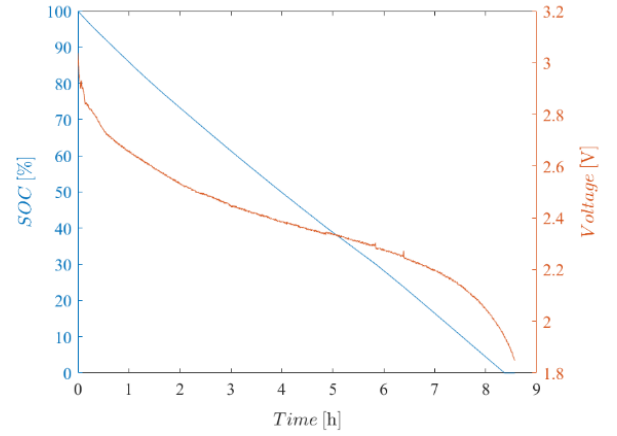


Fig. 11. SOC of AAA alkaline batteries with 110 mA (21°C).

On the other hand, AAA and AA lithium iron disulfide batteries have an approximate capacity of 1300 mAh and 3500 mAh, respectively, and in the range of the project's current measurement, the discharge current does not influence the capacity of these batteries. As illustrated in Fig. 12, on an AAA lithium battery, the estimated capacity is approximately equal to the nominal capacity when discharging at 110 mA.

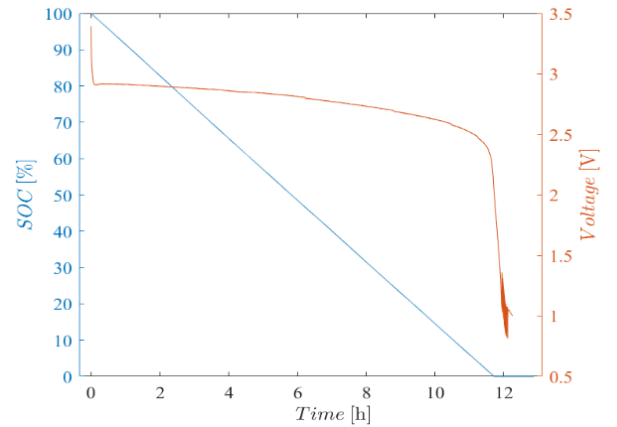


Fig. 12. SOC of AAA LiFe batteries with 110 mA (21°C).

Finally, another type of test was made regarding the operational temperature of these batteries. As expected, the alkaline batteries have a much higher impact on temperature than lithium iron disulfide. The Fig. 13 illustrates one of the tests made on an AA alkaline battery placed inside a freezer at -18°C where it lasted just over ten hours compared to over twenty hours when exposed to room temperature (21°C) with approximately the same discharging current.

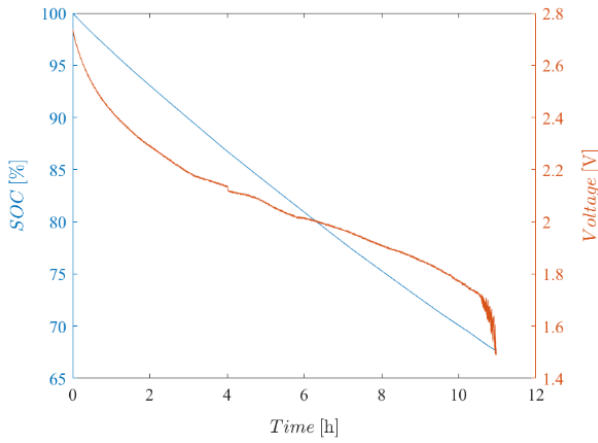


Fig. 13. SOC of AA alkaline batteries with 110 mA (-18°C).

As for the lithium iron disulfide AA batteries, it performed almost the same as when exposed to room temperature. The Fig. 14 illustrates the AA lithium batteries at room temperature and the Fig. 15 illustrates other AA lithium batteries when securely sealed inside a freezer at -18°C.

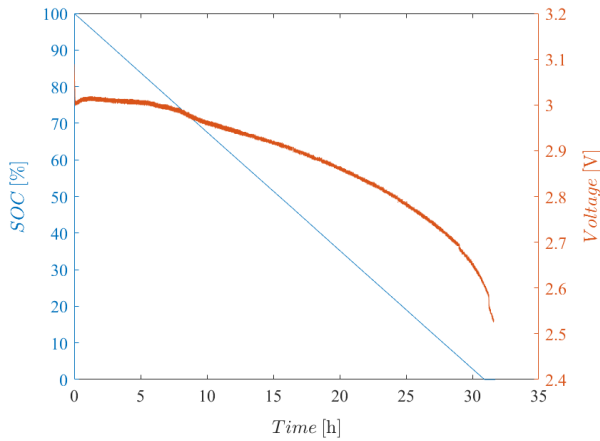


Fig. 14. SOC of AA LiFe batteries with 110 mA (21°C).

Then, in the -18°C SOC test in Fig. 15, it can be noticed that the batteries discharged fully contrarily to the alkaline batteries that still had charge when exposed back to room temperature.

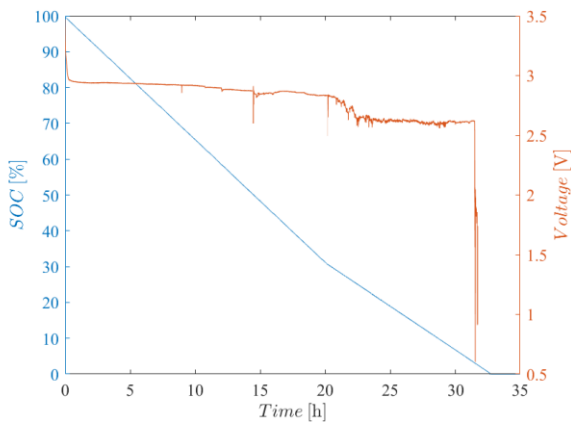


Fig. 15. SOC of AA LiFe batteries with 110 mA (-18°C).

Even though the batteries were more irregular compared to the room temperature results, they could deliver the same voltages as promised by the manufacturer. Since the performances are the same when exposed to these two different temperatures, this proves that the chemicals inside the lithium iron disulfide batteries have less influence on their chemical reactions than inside an alkaline storage device in these operational conditions.

VI. CONCLUSIONS

A new SOC Coulomb counting measurement system for alkaline and lithium iron disulfide batteries was presented. The architecture allows the measurements of currents between the range of 1 to 110 mA at room temperatures for errors below 3% at a production cost of under 10€. This approach replaced the ADC component and was able to equally measure the current by integrating and relate it with the time between pulses not compromising the accuracy of the measurement, power consumption and production cost. By linking the SOC with the OCV measurements, this project brings more assurance in the system by having more comparable data.

The achieved goals of the project in the validation results show the expected battery behaviors in different conditions and demonstrate the accuracy of the measurement with side-by-side graphical representation of the OCV of the developed circuit. Multiple tests on the batteries were made to have more conclusions about the capabilities of the Coulomb counting method. The completed measurements show the success of the project's objectives on measuring current, especially for the efficiency, low cost production and for not noticeably influencing the battery's performance.

REFERENCES

- [1] M. Forsyth and A. Bhatt, "How a battery works - Curious," *www.science.org.au*, 2016. <https://www.science.org.au/curious/technology-future/batteries> (accessed Feb. 19, 2021).
- [2] Energizer, "Cylindrical Primary Lithium Handbook and Application Manual," 2018. https://data.energizer.com/pdfs/lithiuml91192_appman.pdf (accessed Jun. 29, 2021).
- [3] P. Shen, M. Ouyang, L. Lu, J. Li, and X. Feng, "The co-estimation of state of charge, state of health, and state of function for lithium-ion batteries in electric vehicles," *IEEE Transactions on Vehicular Technology*, 2018.
- [4] W.-Y. Chang, M. Brünig, and E. Di Nardo, "The State of Charge Estimating Methods for Battery: A Review Academic Editors," Hindawi Publishing Corporation, 2013. doi: 10.1155/2013/953792.
- [5] REI, "How to Choose Batteries | REI Co-op." <https://www.rei.com/learn/expert-advice/batteries.html> (accessed Jun. 29, 2021).
- [6] Quora, "Why cant you use a AAAA Battery instead of 2 AA Batteries.? - Quora." <https://www.quora.com/Why-cant-you-use-a-AAAA-Battery-instead-of-2-AA-Batteries> (accessed Jun. 30, 2021).